

Quasi-Clique Discovery via Energy Diffusion

Yu Zhang^{1,2}, Yilong Luo^{1,2}, Mingyuan Ma^{1,2}, Yao Chen³, Enqiang Zhu⁴, Jin Xu^{1,2*}, Chanjuan Liu⁵

¹School of Computer Science, Peking University, Beijing, China

²Key Lab of High Confidence Software Technologies, Ministry of Education, Beijing, China

³Information Technology Department, Beijing Capital International Airport Co., Ltd., Beijing, China

⁴Institute of Computing Science and Technology, Guangzhou University, Guangzhou, China

⁵School of Computer Science and Technology, Dalian University of Technology, Dalian, China

{yuzhang.cs, yilong.luo}@stu.pku.edu.cn, zhuenqiang@gzhu.edu.cn, chanjuanliu@dlut.edu.cn

Abstract

Discovering quasi-cliques—subgraphs with edge density no less than a given threshold—is a fundamental task in graph mining, with broad applications in social networks, bioinformatics, and e-commerce. Existing heuristics often rely on greedy rules, similarity measures, or metaheuristic search, but struggle to maintain both efficiency and solution consistency across diverse graphs. This paper introduces EDQC, a novel quasi-clique discovery algorithm inspired by energy diffusion. Instead of explicitly enumerating candidate subgraphs, EDQC performs stochastic energy diffusion from source vertices, naturally concentrating energy within structurally cohesive regions. The approach enables efficient dense subgraph discovery without exhaustive search or dataset-specific tuning. Experimental results on 30 real-world datasets demonstrate that EDQC consistently discovers larger quasi-cliques than state-of-the-art baselines on the majority of datasets, while also yielding lower variance in solution quality. To the best of our knowledge, EDQC is the first method to incorporate energy diffusion into quasi-clique discovery.

Introduction

Dense subgraph models play a fundamental role in network analysis (Pattillo, Youssef, and Butenko 2013), with applications spanning social network mining (Chen and Saad 2010), protein complex detection (Swarnkar et al. 2015), e-commerce recommendation (Song et al. 2021), telecommunications (Wu and Hao 2015), and fraud detection (Fang, Luo, and Ma 2022). Among these models, cliques represent the most stringent form, requiring that every pair of vertices be directly connected to each other. However, due to noise and missing links in real-world networks, exact cliques are rarely observed. To relax this strict requirement, a variety of approximate dense subgraph models have been proposed, including quasi-cliques, k -clubs, and k -plexes. In particular, the γ -quasi-clique—defined by a minimum edge density threshold—has emerged as one of the most widely adopted formulations (Chen et al. 2021; Pang, Ma, and Fang 2024).

Given an undirected graph G and a threshold $\gamma \in (0, 1]$, the Maximum Quasi-Clique Problem (MQCP) seeks the largest vertex set S such that the induced subgraph $G[S]$ exhibits an edge density of at least γ . This edge-density

criterion provides a more direct measure of structural cohesion compared to the degree-based definitions utilized by methods such as FastQC (Konar and Sidiropoulos 2024) and IterQC (Xia et al. 2025). However, the MQCP is NP-hard even for fixed values of γ (Pattillo et al. 2013) and does not possess the hereditary property that allows for efficient pruning in problems related to cliques. Nonetheless, quasi-clique discovery remains highly valuable, as real-world networks typically exhibit dense yet incomplete connectivity rather than perfect cliques, making quasi-cliques crucial for identifying significant or anomalous substructures.

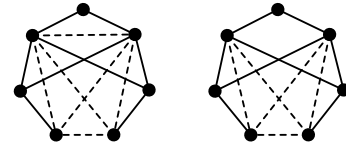


Figure 1: A clique and a 0.8-quasi-clique.

One practical application of quasi-clique discovery is financial fraud detection, where fraud rings form dense but incomplete transaction patterns. Modeling these as γ -quasi-cliques enables the effective identification of suspicious groups under noise and missing links (Jiang et al. 2022). As shown in Figure 1, the *dashed* edges in the left subgraph form a size-4 clique, representing full collusion. In the right subgraph, the dashed edges form a 0.8-quasi-clique—still suspicious, despite one missing link—capturing fraud under partial observation or evasion.

Despite their practical success, identifying quasi-cliques in real-world scenarios such as fraud detection remains computationally challenging, largely due to the enormous scale and inherent complexity of real-world networks. While exact algorithms for MQCP, typically based on integer programming or techniques such as branch-and-bound (Uno 2010; Pastukhov et al. 2018; Ribeiro and Riveaux 2019; Rahman et al. 2024), guarantee optimal solutions, their exponential time complexity restricts their applicability to large-scale networks. As a practical alternative, numerous heuristic methods have been proposed to enable scalable quasi-clique discovery, which can be roughly grouped into four categories. First, greedy expansion techniques, such

*Corresponding authors

as the greedy strategy with local refinement introduced in Tsourakakis et al. (2013) and the restart-enabled search in RIG* (Oliveira, Plastino, and Ribeiro 2013), prioritize speed but are vulnerable to becoming trapped in local optima. Second, metaheuristic frameworks like TSQC (Djeddi, Ait Haddadene, and Belacel 2019) and OBMA (Zhou, Benlic, and Wu 2020) employ tabu search and opposition-based learning, offering enhanced robustness at a higher computational cost. Third, local search algorithms, including NuQClq (Chen et al. 2021) and its variants NuQClqF1 and NuQClqR1 (Liu et al. 2024), utilize bounded configuration checking and adaptive rules for candidate refinement. However, despite their sophisticated local optimizations, these methods often exhibit instability due to their dependence on random number generator seeds. Lastly, similarity-based heuristics such as NBSim and its accelerated variant, FastNBSim, utilize vertex neighborhood overlap to identify and expand quasi-cliques (Pang, Ma, and Fang 2024). While both methods are highly efficient, FastNBSim introduces MinHash-based approximations, making it sensitive to random number generator seeds and potentially less stable. Moreover, neither method explicitly supports a user-defined density threshold. Instead, the resulting subgraph density emerges implicitly from similarity parameters, which makes them unsuitable for applications requiring strict control over quasi-clique density thresholds. Among the four heuristic categories, local search and similarity-based methods have been the most competitive for discovering large quasi-cliques, yet they remain sensitive to random initialization and lack explicit density control. In particular, the state-of-the-art algorithms for MQCP include NBSim and its accelerated variant, FastNBSim (Pang, Ma, and Fang 2024), as well as the local search algorithms NuQClqF1 and NuQClqR1 (Liu et al. 2024).

Energy diffusion offers a promising alternative paradigm. Diffusion-based techniques such as PageRank (Page et al. 1999) and the heat kernel (Chung 2007) have demonstrated strong performance in structure-aware tasks like vertex ranking and community detection (Kloster and Gleich 2014; Gleich, Lim, and Yu 2015), where information tends to concentrate in cohesive regions. This property aligns naturally to identify dense subgraphs. However, to the best of our knowledge, energy diffusion has not yet been explored for quasi-clique discovery, despite its strong alignment with the structural objectives of the task. This gap suggests an opportunity to design methods that identify dense subgraphs by leveraging the natural tendency of diffusion processes to concentrate within cohesive regions.

To address this gap, we introduce Energy Diffusion-Driven Quasi-Clique Discovery (EDQC), a novel and robust algorithm that leverages energy diffusion as its core mechanism for efficiently identifying quasi-cliques. EDQC simulates stochastic diffusion from energy sources, naturally accumulating energy in structurally cohesive regions. Rather than relying on explicit subgraph enumeration, it extracts quasi-cliques through a spectral criterion that reflects the energy distribution across the graph. This diffusion-driven process implicitly favors denser subgraphs, contributing to stable results across

random seeds and reducing sensitivity to parameter settings. Experiments on 30 representative real-world datasets show that EDQC yields consistently high solution quality with low variance, while maintaining competitive runtime.

Problem Definition

In this paper, all graphs under consideration are undirected and do not contain loops or parallel edges. Let $G = (V, E)$ represent a graph with a *vertex set* V and an *edge set* E . Two vertices u and v within V are termed *adjacent* if $uv \in E$, and one vertex is referred to as a *neighbor* of the other. The set of all neighbors for a vertex u is known as its *neighborhood*, denoted $N(u)$, while the *closed neighborhood* of u is denoted $N[u] = N(u) \cup \{u\}$. The *degree* of a vertex u , denoted as $d(u)$, indicates the number of its neighbors, i.e., $d(u) = |N(u)|$. For any subset of vertices $S \subseteq V$, the *induced subgraph* on S , denoted by $G[S]$, consists of the vertex set S and the edge set $\{uv \in E \mid u, v \in S\}$. The *edge density* of G , denoted as $\eta(G)$, is defined by the formula

$$\eta(G) = \frac{|E|}{\binom{|V|}{2}},$$

where $\binom{|V|}{2}$ represents the maximum number of possible edges among the vertices in V .

Definition 1 (γ -Quasi-Clique). *Let $G = (V, E)$ be a graph and $\gamma \in (0, 1]$ a positive real number. A subset of vertices $S \subseteq V$ is referred to as a γ -quasi-clique of G if the edge density of the induced subgraph $G[S]$ satisfies $\eta(G[S]) \geq \gamma$, with γ serving as the density threshold. A γ -quasi-clique is considered maximal if there is no larger subset of vertices $S' \subseteq V$ such that $S \subset S'$ and S' is also a γ -quasi-clique.*

Definition 2 (Maximum Quasi-Clique Problem (MQCP)). *Given a graph $G = (V, E)$ and a density threshold $\gamma \in (0, 1]$, the Maximum Quasi-Clique Problem (MQCP) seeks to identify a γ -quasi-clique S^* with the maximum cardinality. Specifically,*

$$S^* = \arg \max_{S \subseteq V} \{|S| \mid \eta(G[S]) \geq \gamma\}.$$

When $\gamma = 1$, the MQCP reduces to the classic Maximum Clique Problem. For any fixed γ , the MQCP is NP-hard and may have multiple optimal solutions (Pattillo et al. 2013).

Energy Diffusion-Driven Quasi-Clique Discovery

We propose a diffusion-based algorithm in which each vertex acts as an energy source, initiating stochastic diffusion across the graph. This physically inspired process tends to concentrate energy in densely connected regions due to enhanced *energy retention*, facilitating the efficient identification of quasi-cliques. Our approach is conceptually related to spectral and diffusion-based methods, such as Graph Diffusion Convolution (GDC), which similarly foster locality and structural cohesion (Gasteiger, Weißenberger, and Günnemann 2019).

Algorithm 1: EDQC(G, γ, T, θ)

Input: Graph $G = (V, E)$, density threshold γ , diffusion steps T , activation threshold θ

Output: A quasi-clique Q^*

```
1  $Q^* \leftarrow \emptyset$ ;  
2 foreach  $v \in V$  in non-increasing order of degree do  
3    $f \leftarrow \text{ENERGYDIFFUSION}(G, v, T, \theta)$ ;  
4    $Q \leftarrow \text{EXTRACTQUASICLIQUE}(G, f, \gamma, \theta)$ ;  
5   if  $|Q| > |Q^*|$  then  
6      $Q^* \leftarrow Q$ ;  
7 return  $Q^*$ 
```

Algorithm Overview

Algorithm 1 outlines the core procedure of EDQC. Given a graph $G = (V, E)$ and a density threshold γ , the algorithm processes the vertices in non-increasing order of degree, treating each in turn as an energy source, simulates energy diffusion to obtain an energy map $f : V \rightarrow \mathbb{R}$ (line 3), and extracts a high-density subgraph guided by this signal (line 4). If the size of the extracted subgraph surpasses that of the current best, it becomes the new best solution (lines 5–6). After all vertices have been processed, the largest quasi-clique found is returned (line 7).

Energy Diffusion Process

We utilize the ENERGYDIFFUSION procedure (Algorithm 2) to compute an energy map $f : V \rightarrow \mathbb{R}$, where $f(x)$ denotes the energy assigned to vertex x after diffusion from a specified energy source v .

The energy map f is initialized by assigning unit energy to the source vertex v , with all other vertices initialized to zero. An active vertex set $A \subseteq V$ is maintained throughout the process, initially containing only v (line 1). This set consists of vertices currently eligible to diffuse energy, i.e., those with energy values exceeding the activation threshold.

During each of the T diffusion steps, the algorithm updates f by simulating energy transfer from each active vertex $u \in A$ to its neighbors (lines 2–9). For each neighbor $w \in N(u)$, a positive random weight ω_{uw} is generated and normalized across all neighbors of u such that the weights sum to one (lines 4–5). Each neighbor w then receives a portion of $f(u)$, proportional to ω_{uw} and scaled by a diffusion factor of $\frac{1}{2}$ (lines 6–7). Once all neighbors have been updated, the energy of vertex u is halved (line 8). This local update process can be formally characterized by the following equation:

$$f(w) = \begin{cases} f(w) & \text{if } w \notin N[u] \\ \frac{f(w)}{2} & \text{if } w = u \\ f(w) + \frac{f(u)}{2} \cdot \omega_{uw} & \text{if } w \in N(u) \end{cases} \quad (1)$$

This update rule reflects a single local diffusion step centered at the vertex u , modifying the energy distribution across its 1-hop neighborhood.

After all active vertices have been processed, the active set A is updated to include only those vertices with energy values exceeding the threshold θ (line 9). After T iterations, the final energy map f is returned (line 10).

Algorithm 2: ENERGYDIFFUSION(G, v, T, θ)

Input: Graph $G = (V, E)$, energy source vertex v , diffusion steps T , activation threshold θ

Output: An energy map $f : V \rightarrow \mathbb{R}$

```
1  $f(v) \leftarrow 1, f(u) \leftarrow 0$  for all  $u \neq v$ ;  $A \leftarrow \{v\}$ ;  
2 for  $t = 1$  to  $T$  do  
3   foreach  $u \in A$  do  
4     Generate weights  $\omega_{uw} > 0$  for  $w \in N(u)$ ;  
5     Normalize  $\omega_{uw}$  such that  $\sum_{w \in N(u)} \omega_{uw} = 1$ ;  
6     foreach  $w \in N(u)$  do  
7        $f(w) \leftarrow f(w) + \frac{f(u)}{2} \cdot \omega_{uw}$ ;  
8      $f(u) \leftarrow \frac{f(u)}{2}$ ;  
9    $A \leftarrow \{v \in V \mid f(v) > \theta\}$ ;  
10 return  $f$ 
```

We observe that denser regions tend to retain more energy during diffusion, likely due to their higher internal connectivity. This intuition is supported by an empirical analysis of 1,000 equal-sized vertex subsets, which shows a strong positive correlation between subgraph density and energy retention, as demonstrated in our experiments.

Lemma 1. *Let $G = (V, E)$ be a graph, and let $f^{(i)} : V \rightarrow \mathbb{R}$ denote the energy map after the i th diffusion round in Algorithm 2. Then, for all i ,*

$$\sum_{x \in V} f^{(i)}(x) = 1.$$

Proof. Initially, only the source vertex is assigned energy 1, and all others are 0, resulting in a total energy of 1 across all vertices. Therefore, it is sufficient to demonstrate that the total energy across all vertices remains unchanged in each iteration. To establish this, we need to show that the sum of the energies of each vertex u and its neighbors remains constant before and after the energy diffusion process between u and its neighborhood $N(u)$. Let $f^{(i)}$ and $f^{(i+1)}$ represent the energy maps before and after the i th round, where $i \in \{0, 1, \dots, T-1\}$. According to the diffusion rule outlined in Equation 1, we have

$$\begin{aligned}
& \sum_{x \in N[u]} f^{(i+1)}(x) \\
&= f^{(i+1)}(u) + \sum_{x \in N(u)} f^{(i+1)}(x) \\
&= \frac{f^{(i)}(u)}{2} + \sum_{x \in N(u)} \left(f^{(i)}(x) + \frac{f^{(i)}(u)}{2} \cdot \omega_{xu} \right) \\
&= \frac{f^{(i)}(u)}{2} + \sum_{x \in N(u)} f^{(i)}(x) + \frac{f^{(i)}(u)}{2} \sum_{x \in N(u)} \omega_{xu} \\
&= \sum_{x \in N[u]} f^{(i)}(x)
\end{aligned}$$

□

Lemma 1 confirms that the energy diffusion process conserves total energy at each iteration. This ensures that the resulting energy map is a redistribution of the initial input, providing stability and fairness across different source vertices.

Theorem 1. *The time complexity of Algorithm 2 is $O(Tn\Delta)$, where T is the diffusion step count, $n = |V|$ is the number of vertices, and Δ is the maximum vertex degree.*

Proof. The algorithm first sorts all vertices by non-increasing degree, which takes $O(n + \Delta)$ time using bucket sort. In each of the T diffusion steps, all n vertices may become active, and each may update up to Δ neighbors, leading to $O(n\Delta)$ time per step. Hence, the total time complexity is $O(Tn\Delta)$. □

Energy-Guided Subgraph Extraction

First, the active vertex set $A \subseteq V$ is reconstructed from the input energy map f and activation threshold θ , as $A = \{v \in V \mid f(v) \geq \theta\}$ (line 1). The vertices in A are then sorted in descending order of energy (line 2). A spectral breakpoint b is identified as the index corresponding to the largest energy drop in the ordered sequence, specifically $b = \arg \max_i (f(v_i) - f(v_{i+1}))$, thereby defining the high-energy prefix (line 3). The top b vertices constitute the initial candidate set S (line 4). If the density of $G[S]$ falls below the threshold γ and the size of S exceeds 3, the least energetic vertices are iteratively removed until either the density constraint is met or S becomes too small (lines 5–6), as tiny subgraphs are typically uninformative in practice. If S remains insufficiently dense, the procedure terminates and returns \emptyset (lines 7–8). Otherwise, vertices from $A \setminus S$ are greedily reinserted in order of energy, as long as the density constraint is maintained (lines 9–11). The resulting subgraph $G[S]$ is then returned as the quasi-clique (line 12).

Theorem 2. *Let $n = |V|$ be the total number of vertices and $k = |A|$ the number of active vertices. Then the time complexity of EXTRACTQUASICLIQUE is $O(n + k^2)$.*

Proof. The algorithm first constructs the active vertex set $A = \{v \in V \mid f(v) \geq \theta\}$ by scanning all vertices, which

Algorithm 3: EXTRACTQUASICLIQUE(G, f, γ, θ)

Input: Graph $G = (V, E)$, energy map $f : V \rightarrow \mathbb{R}$, density threshold γ , activation threshold θ

Output: A γ -quasi-clique Q

```

1  $A \leftarrow \{v \in V \mid f(v) \geq \theta\}$ ;
2 Sort  $A$  by decreasing  $f(v)$ ;
3 Find index  $b$  with largest energy drop;
4  $S \leftarrow$  the top- $b$  vertices in  $A$ ;
5 while  $|S| > 3$  and  $\eta(G[S]) < \gamma$  do
6    $\lfloor$  Remove the last vertex from  $S$ 
7 if  $\eta(G[S]) < \gamma$  then
8    $\lfloor$  return  $\emptyset$ 
9 foreach  $v \in A \setminus S$  in order do
10   $\lfloor$  if  $\eta(G[S \cup \{v\}]) \geq \gamma$  then
11     $\lfloor$   $S \leftarrow S \cup \{v\}$ 
12 return  $G[S]$ 

```

takes $O(n)$ time. Subsequent computations depend only on A , and we analyze them in terms of $k = |A|$. The set A is sorted in descending energy, requiring $O(k \log k)$ time. Computing the spectral breakpoint and initializing the candidate set take $O(k)$ time. The main cost lies in the density-based refinement: in the worst case, up to k vertices may be removed or reinserted. Each update checks the density of $G[S]$, which may require scanning $O(k^2)$ potential edges. Thus, the overall worst-case complexity is $O(n + k^2)$. □

Experimental Evaluation

We conducted comprehensive experiments on real-world datasets to evaluate the performance and robustness of EDQC. This section first describes the experimental setup, followed by the datasets and baseline methods. We then present the main results, provide an empirical analysis of energy retention in dense subgraphs, and conclude with parameter sensitivity and ablation studies.

Experimental Setup

All methods were implemented in C++ and compiled with g++ 9.4.0 using the ‘-O3’ optimization flag. Experiments were conducted on a machine equipped with an AMD EPYC 7H12 CPU (1.5 GHz base frequency) and 944 GB of RAM, running Ubuntu 20.04 with Linux kernel 5.4.0.

Each baseline algorithm was run with the parameter settings recommended in its original paper. For EDQC, we set the diffusion step count to $T = 3$ and the activation threshold to $\theta = 0.001$, based on a parameter sensitivity analysis across datasets of varying scales (see the section on parameter sensitivity), where these values consistently yielded competitive performance. Due to inherent randomness, all methods except NBSim were executed 10 times with random seeds from 1 to 10; NBSim is deterministic and thus evaluated only once. We report the average quasi-clique size within a 60-second timeout, standard deviation (if applicable), runtime, and significance via one-tailed paired t -tests. The 60-second timeout reflects common practice in recent time-bounded heuristic search studies (Lin et al. 2017;

Datasets

We evaluated EDQC on 30 datasets from SNAP (Leskovec and Krevl 2014) and the Network Repository (Rossi and Ahmed 2015), covering diverse domains such as social, collaboration, communication, web, and synthetic networks. These datasets range from thousands to over 16 million vertices, with edge densities spanning from 10^{-2} to 10^{-6} . Table 1 summarizes the number of vertices (n), edges (m), and edge density for each network. The diversity in size and sparsity makes this collection a realistic and challenging testbed for evaluating the scalability and effectiveness of quasi-clique discovery algorithms.

Dataset	n	m	Density
ego-facebook	4039	88234	1.08×10^2
CA-GrQc	5241	14484	1.05×10^3
CA-HepPh	12006	118489	1.64×10^3
CA-CondMa	23133	93439	3.49×10^4
Email-Enron	36692	183831	2.73×10^4
cond-mat-2005	39577	175693	2.24×10^4
wordnet-words	73753	234024	8.60×10^5
yahoo-msg	100058	739815	1.48×10^4
luxembourg_osm	114599	119666	1.82×10^5
rgg_n.2.17_s0	131070	728753	8.48×10^5
Loc-Gowalla	196591	950327	4.92×10^5
coAuthorsCiteseer	227320	814134	3.15×10^5
delaunay_n18	262144	786396	2.29×10^5
web-Stanford	281903	1992636	5.01×10^5
coAuthorsDBLP	299067	977676	2.19×10^5
com-dblp	317080	1049866	2.09×10^5
web-NotreDame	325729	1090108	2.05×10^5
com-amazon	334863	925872	1.65×10^5
rgg_n.2.19_s0	524284	3269766	2.38×10^5
coPapersDBLP	540486	15245729	1.04×10^4
web-BerkStan	685230	6649470	2.83×10^5
eu-2005	862664	16138468	4.34×10^5
web-Google	875713	4322051	1.13×10^5
rgg_n.2.20_s0	1048575	6891620	1.25×10^5
in-2004	1382867	13591473	1.42×10^5
rgg_n.2.21_s0	2097148	14487995	6.59×10^6
rgg_n.2.22_s0	4194301	30359198	3.45×10^6
rgg_n.2.23_s0	8388607	63501393	1.80×10^6
rgg_n.2.24_s0	16777215	132557200	9.42×10^7
delaunay_n24	16777216	50331601	3.58×10^7

Table 1: Summary of evaluation datasets.

Baseline Methods

We compare EDQC with four recent state-of-the-art quasi-clique discovery algorithms:

- NBSim/FastNBSim (Pang, Ma, and Fang 2024): similarity-driven heuristics that expand subgraphs based on neighborhood overlap. FastNBSim accelerates NBSim via MinHash-based approximation.
- NuQClqF1/NuQClqR1 (Liu et al. 2024): advanced variants of NuQClq (Chen et al. 2021). These algorithms employ information feedback models that integrate historical solutions using fitness-weighted scores to guide local search.

Main Results

We report the average size and standard deviation of quasi-cliques discovered by each algorithm under different density thresholds γ . In Table 2, γ is set according to the density of NBSim’s output; in Table 3, γ is set to the highest sub-graph density achieved by FastNBSim across 10 runs, favoring quasi-cliques of higher structural cohesion.

Dataset	γ	NBSim	NuQClqF1	NuQClqR1	EDQC
ego-facebook	0.99	71	92	92	89.2±0.60
CA-GrQc	0.99	46	46	46	46
CA-HepPh	1	239	239	239	239
CA-CondMa	1	26	26	26	26
Email-Enron	0.97	10	25	25	22.3±0.90
cond-mat-2005	1	30	30	30	30
wordnet-words	1	32	32	32	32
yahoo-msg	0.99	22	20.2±2.04 ^b	20.6±1.91 ^b	23
luxembourg_osm	1	3	3	3	3
rgg_n.2.17_s0	1	15	15	15	15
Loc-Gowalla	0.99	31	23.8±2.40 ^c	23 ^c	31
coAuthorsCiteseer	1	87	87	87	87
delaunay_n18	1	4	4	4	4
web-Stanford	0.99	67	64.2±3.25 ^b	60.2±42 ^c	68
coAuthorsDBLP	1	115	115	115	115
com-dblp	1	114	114	114	114
web-NotreDame	1	155	154.3±0.46 ^c	154.2±0.40 ^c	155
com-amazon	1	7	7	7	7
rgg_n.2.19_s0	0.99	19	19	19	19
coPapersDBLP	1	337	333.5±3.91 ^a	333.5±3.91 ^a	337
web-BerkStan	0.99	202	121.4±47.20 ^c	119.7±39.67 ^c	202
eu-2005	0.99	405	191.3±109.90 ^c	127.2±25.54 ^c	406
web-Google	0.99	48	39.2±7.45	39.5±73	42
rgg_n.2.20_s0	0.57	17	41	41	41
in-2004	0.99	492	494	494	494
rgg_n.2.21_s0	1	18	18.1±0.54 ^c	18.1±0.54 ^c	19
rgg_n.2.22_s0	1	19	18.9±0.70 ^c	18.7±0.64 ^c	19.9±0.30
rgg_n.2.23_s0	0.99	19	18.3±0.46 ^c	19±1.34 ^c	21.8±0.60
rgg_n.2.24_s0	0.98	20	19.7±0.90 ^c	18.7±0.46 ^c	23
delaunay_n24	1	4	4	4	4

Table 2: Quasi-clique sizes (γ from NBSim).

For each dataset, the largest average size is highlighted in bold. EDQC achieves the best or nearly best performance across almost all datasets, while also exhibiting lower standard deviations, indicating more stable results across runs. In contrast, NuQClqF1 and NuQClqR1 often show larger standard deviations due to randomness in their search process.

Statistical significance is assessed via one-tailed paired t -tests comparing EDQC against NuQClqF1 and NuQClqR1. Superscripts ^a, ^b, and ^c are appended to the NuQClqF1 and NuQClqR1 columns to denote results significantly worse than EDQC at the $p < 0.05$, $p < 0.01$, and $p < 0.001$ levels, respectively. NBSim is excluded from significance testing due to its deterministic nature, and FastNBSim is excluded because it may return subgraphs that do not strictly satisfy the density constraint γ . Overall, EDQC consistently discovers larger quasi-cliques with lower variance and statistically significant improvements over the strongest non-deterministic baselines, confirming its robustness and effectiveness across diverse network scenarios.

Figure 2 presents the average runtime of all five algorithms across the 30 datasets. To unify the comparison,

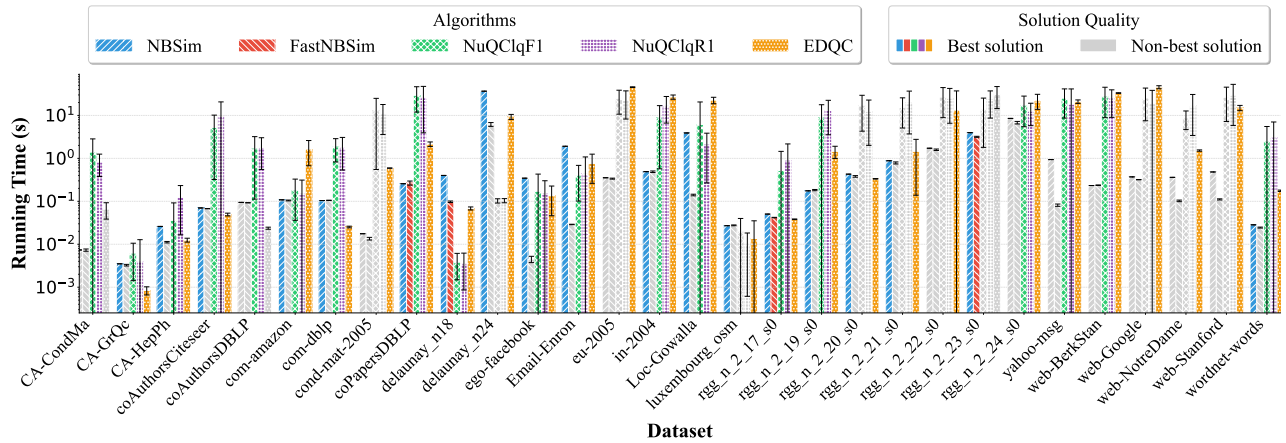


Figure 2: Efficiency of five algorithms.

Dataset	γ	FastNBSim	NuQClqF1	NuQClqR1	EDQC
ego-facebook	0.96	97.2±9.47	123	123	118.7±0.78
CA-GrQc	1	38.9±3.42	44	44	44
CA-HepPh	1	173.4±621	239	239	239
CA-CondMa	1	22.5±2.84	26	26	26
Email-Enron	0.96	16.5±1.28	26	26	23.8±0.98
cond-mat-2005	1	27.6±3.10	30	30	30
wordnet-words	1	28.9±2.26	32	32	32
yahoo-msg	0.96	22.2±1.78	22.9±1.92 ^c	23.7±1.00 ^b	25
luxembourg_osm	1	3	3	3	3
rgg_n_2_17_s0	0.99	15.6±0.80	15	15	15
Loc-Gowalla	1	28.4±37	21 ^c	21 ^c	29
coAuthorsCiteseer	1	81.6±58	87	87	87
delaunay_n18	0.7	5.1±0.30	6	6	6
web-Stanford	0.99	64±3.32	64.2±3.25 ^c	60.1±41 ^c	68
coAuthorsDBLP	1	103±9.20	115	115	115
com-dblp	1	101.4±5.46	114	114	114
web-NotreDame	1	153.5±1.36	154.3±0.46 ^c	154.2±0.40 ^c	155
com-amazon	1	7.1±0.54	7	7	7
rgg_n_2_19_s0	0.99	17.4±0.80	19	19	19
coPapersDBLP	1	316.9±21.82	333.5±3.91 ^a	331.4±97 ^a	337
web-BerkStan	1	191.5±10.98	120.7±30.97 ^c	113.5±38.46 ^c	201
eu-2005	0.99	401.4±4.92	191.3±109.90 ^c	127.2±25.54 ^c	406
web-Google	1	44.8±44	33.7±2.49 ^c	37.1±5.77	38
rgg_n_2_20_s0	0.99	17.9±0.83	18	18	18
in-2004	0.99	473.3±12.43	494	494	494
rgg_n_2_21_s0	0.98	18.9±0.70	19	19	19
rgg_n_2_22_s0	0.98	19.8±0.87	20.1±0.94 ^b	20±0.89 ^b	21
rgg_n_2_23_s0	0.99	21.7±0.90	18.3±0.46 ^c	19±1.34 ^c	21.8±0.60
rgg_n_2_24_s0	0.95	21.6±0.92	20.6±1.20 ^c	20.9±1.30 ^c	24.9±0.30
delaunay_n24	0.7	5.8±0.60	6	6	6

Table 3: Quasi-clique sizes (γ from FastNBSim).

we aggregate the results under two density thresholds γ , which are respectively derived from the output of NBSim and FastNBSim (as used in Tables 2 and 3). For NuQClqF1, NuQClqR1, and EDQC, we report the average runtime over both settings per dataset, while NBSim and FastNBSim are evaluated only under their respective default γ values.

To ensure fairness, we include runtime bars only for algorithms that achieve the best average quasi-clique size under at least one of the two γ settings for each dataset. Algorithms that fail to reach this benchmark are either omitted or shown with grayed-out bars. This design empha-

sizes the efficiency-performance trade-offs among the methods. The results show that although NBSim and FastNBSim are highly efficient, their solution quality is often inferior. Among the methods that achieve top-quality solutions, EDQC is faster than NuQClqF1 or NuQClqR1 on more datasets. This indicates that EDQC provides the best overall balance between solution quality and runtime, making it a practical and robust choice for quasi-clique discovery.

Correlation Between Density and Energy Retention

To further investigate the relationship between subgraph density and energy retention, we select 8 representative networks from different domains. For each dataset, we randomly choose one quasi-clique discovered by EDQC in a single run (out of 10) and fix its size k . We then randomly generate 1,000 vertex subsets $S \subseteq V$ of size k , and for each subset S , we compute the subgraph density $\eta(G[S])$ and total retained energy $f(S) = \sum_{v \in S} f(v)$, where f is the energy map obtained from the diffusion process.

Figure 3 shows the resulting scatter plots, where each blue point represents one sampled subset. The red mark indicates the quasi-clique identified by EDQC in the selected run. Each plot also reports the Pearson correlation coefficient ($Corr$) between subgraph density and retained energy. The results consistently reveal a strong positive correlation across networks, supporting the intuition that denser regions retain more energy during diffusion. These findings provide empirical evidence for the energy-density alignment underlying EDQC’s design.

Parameter Sensitivity

We analyzed the sensitivity of EDQC to its two key parameters: the diffusion step count T and the activation threshold θ . To this end, we selected three representative datasets of different scales—small, medium, and large—and evaluated EDQC under all combinations of $T \in \{1, 2, 3\}$ and $\theta \in \{0.0001, 0.0005, 0.001, 0.005, 0.01\}$.

The average size of the extracted quasi-cliques was used as the performance metric. The results, shown in Figure 4, indicate that EDQC’s output is sensitive to parameter

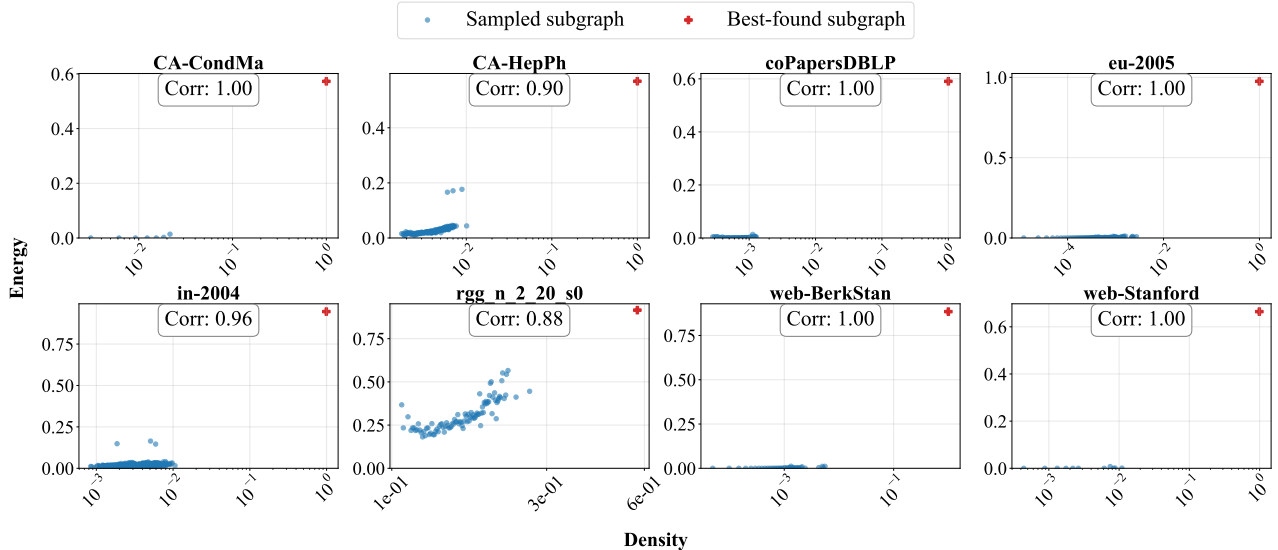


Figure 3: Relationship between Energy and Density.

choices: both the diffusion depth and activation threshold substantially influence performance. In general, larger values of T allow energy to diffuse further, which can improve coverage in loosely connected regions, but also increase runtime due to more iterations of energy updates. Conversely, overly aggressive thresholds may suppress useful diffusion paths, leading to suboptimal subgraphs.

Among all tested configurations, the combination $T = 3$ and $\theta = 0.001$ consistently yielded competitive or near-best results across the selected datasets. We therefore adopt these as the default settings in all experiments.

Ablation Study

To evaluate the impact of key components in EDQC, we conduct an ablation study by systematically removing three design elements: (i) *degree-based vertex ordering*, (ii) *activation thresholding* (i.e., considering all vertices with $f(v) > 0$ as active), and (iii) *spectral breakpoint extraction* (i.e., the top- b truncation in Algorithm 3). For the third variant, we replace Algorithm 3 with a greedy construction strategy: vertices are inserted in descending energy order into the quasi-clique until the density constraint is violated, after which the last inserted vertex is removed to ensure feasibility.

Variant	#Best	#Worst
EDQC (full)	59	0
w/o Seed Ordering	31	20
w/o Activation Threshold	30	22
w/o Spectral Breakpoint	14	42

Table 4: Number of settings (out of 60) where each method achieves the best or worst average quasi-clique size (averaged over 10 runs).

Each variant is evaluated across 30 datasets under two density thresholds (derived from NBSim and FastNBSim

outputs, as in Tables 2 and 3), totaling 60 experimental settings. Table 4 reports the number of cases where each variant achieves either the best or worst average quasi-clique size. The results show that all three components contribute meaningfully to EDQC’s effectiveness. The full EDQC achieves the best result in 59 out of 60 settings and is never the worst performer. The results demonstrate that all key components in EDQC are effective.

Conclusion

This paper introduced EDQC, the first quasi-clique discovery algorithm driven by energy diffusion. By simulating stochastic diffusion processes initiated from energy source vertices, EDQC naturally accumulates energy in structurally cohesive regions, efficiently guiding quasi-clique extraction without exhaustive enumeration. Extensive evaluations on real-world datasets demonstrated that EDQC consistently finds larger and more stable quasi-cliques compared to state-of-the-art heuristics, while maintaining competitive computational efficiency. Ablation study further confirmed the effectiveness of our key design strategies. In future work, we aim to generalize EDQC to weighted and attributed graphs, extending its applicability to complex heterogeneous networks. Another promising direction is incorporating adaptive strategies to further improve solution quality. We also plan to apply EDQC to practical tasks such as community detection, fraud analysis, and bioinformatics, where dense structure discovery is critical.

References

Chen, J.; Cai, S.; Pan, S.; Wang, Y.; Lin, Q.; Zhao, M.; and Yin, M. 2021. NuQClq: An effective local search algorithm for maximum quasi-clique problem. In *Proceedings of the AAAI Conference on Artificial Intelligence*, volume 35, 12258–12266.

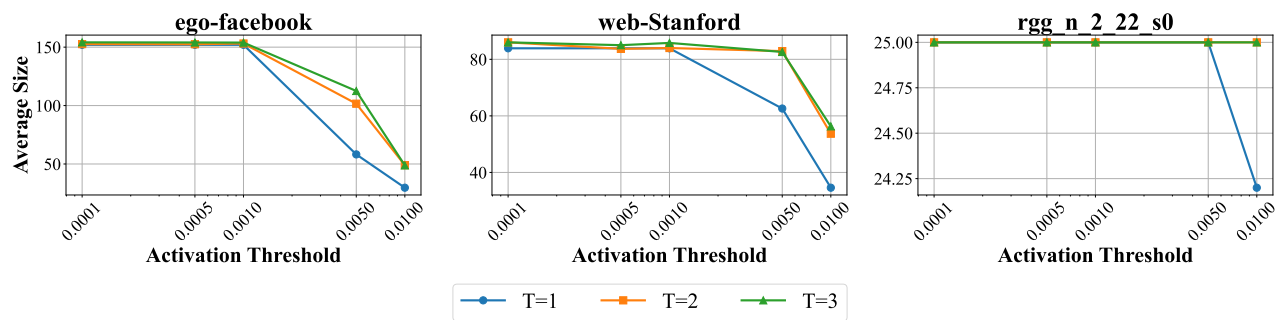


Figure 4: Sensitivity Study of Parameters.

Chen, J.; and Saad, Y. 2010. Dense subgraph extraction with application to community detection. *IEEE Transactions on knowledge and data engineering*, 24(7): 1216–1230.

Chung, F. 2007. The heat kernel as the pagerank of a graph. *Proceedings of the National Academy of Sciences*, 104(50): 19735–19740.

Djeddi, Y.; Ait Haddadene, H.; and Belacel, N. 2019. An extension of adaptive multi-start tabu search for the maximum quasi-clique problem. *Computers & Industrial Engineering*, 132: 280–292.

Fang, Y.; Luo, W.; and Ma, C. 2022. Densest subgraph discovery on large graphs: Applications, challenges, and techniques. *Proceedings of the VLDB Endowment*, 15(12): 3766–3769.

Gasteiger, J.; Weissenberger, S.; and Günnemann, S. 2019. Diffusion improves graph learning. *Advances in neural information processing systems*, 32.

Gleich, D. F.; Lim, L.-H.; and Yu, Y. 2015. Multilinear pagerank. *SIAM Journal on Matrix Analysis and Applications*, 36(4): 1507–1541.

Jiang, J.; Li, Y.; He, B.; Hooi, B.; Chen, J.; and Kang, J. K. Z. 2022. Spade: A real-time fraud detection framework on evolving graphs. *Proceedings of the VLDB Endowment*, 16(3): 461–469.

Kloster, K.; and Gleich, D. F. 2014. Heat kernel based community detection. In *Proceedings of the 20th ACM SIGKDD international conference on Knowledge discovery and data mining*, 1386–1395.

Konar, A.; and Sidiropoulos, N. D. 2024. Optimal quasi-clique: hardness, equivalence with densest-k-subgraph, and quasi-partitioned community mining. In *Proceedings of the AAAI Conference on Artificial Intelligence*, volume 38, 8608–8616.

Leskovec, J.; and Krevl, A. 2014. SNAP Datasets: Stanford Large Network Dataset Collection.

Lin, J.; Cai, S.; Luo, C.; and Su, K. 2017. A Reduction based Method for Coloring Very Large Graphs. In *Proceedings of the 26th International Joint Conference on Artificial Intelligence*, 517–523.

Liu, S.; Zhou, J.; Wang, D.; Zhang, Z.; and Lei, M. 2024. An optimization algorithm for maximum quasi-clique problem based on information feedback model. *PeerJ Computer Science*, 10: e2173.

Oliveira, A.; Plastino, A.; and Ribeiro, C. 2013. Construction heuristics for the maximum cardinality quasi-clique problem. In *10th Metaheuristics International Conference. Singapore*, volume 84.

Page, L.; Brin, S.; Motwani, R.; and Winograd, T. 1999. The PageRank citation ranking: Bringing order to the web. Technical report, Stanford infolab.

Pang, J.; Ma, C.; and Fang, Y. 2024. A Similarity-based Approach for Efficient Large Quasi-clique Detection. In *Proceedings of the ACM Web Conference 2024*, 401–409.

Pastukhov, G.; Veremyev, A.; Boginski, V.; and Prokopyev, O. A. 2018. On maximum degree-based-quasi-clique problem: Complexity and exact approaches. *Networks*, 71(2): 136–152.

Pattillo, J.; Veremyev, A.; Butenko, S.; and Boginski, V. 2013. On the maximum quasi-clique problem. *Discrete Applied Mathematics*, 161(1-2): 244–257.

Pattillo, J.; Youssef, N.; and Butenko, S. 2013. On clique relaxation models in network analysis. *European Journal of Operational Research*, 226(1): 9–18.

Rahman, A.; Roy, K.; Maliha, R.; and Chowdhury, T. F. 2024. A Fast Exact Algorithm to Enumerate Maximal Pseudo-cliques in Large Sparse Graphs. In *Proceedings of the 30th ACM SIGKDD Conference on Knowledge Discovery and Data Mining*, 2479–2490.

Ribeiro, C. C.; and Riveaux, J. A. 2019. An exact algorithm for the maximum quasi-clique problem. *International Transactions in Operational Research*, 26(6): 2199–2229.

Rossi, R. A.; and Ahmed, N. K. 2015. The Network Data Repository with Interactive Graph Analytics and Visualization. In *AAAI*.

Song, J.; Qu, X.; Hu, Z.; Li, Z.; Gao, J.; and Zhang, J. 2021. A subgraph-based knowledge reasoning method for collective fraud detection in E-commerce. *Neurocomputing*, 461: 587–597.

Swarnkar, T.; Simoes, S. N.; Anura, A.; Brentani, H.; Chatterjee, J.; Hashimoto, R. F.; Martins, D. C.; and Mitra, P. 2015. Identifying dense subgraphs in protein–protein interaction network for gene selection from microarray data. *Network Modeling Analysis in Health Informatics and Bioinformatics*, 4: 1–18.

- Tsourakakis, C.; Bonchi, F.; Gionis, A.; Gullo, F.; and Tsiarli, M. 2013. Denser than the densest subgraph: extracting optimal quasi-cliques with quality guarantees. In *Proceedings of the 19th ACM SIGKDD international conference on Knowledge discovery and data mining*, 104–112.
- Uno, T. 2010. An efficient algorithm for solving pseudo clique enumeration problem. *Algorithmica*, 56: 3–16.
- Wu, Q.; and Hao, J.-K. 2015. A review on algorithms for maximum clique problems. *European Journal of Operational Research*, 242(3): 693–709.
- Xia, H.; Yu, K.; Liu, S.; Long, C.; and Zhou, X. 2025. Maximum Degree-Based Quasi-Clique Search via an Iterative Framework. *Proceedings of the 31th ACM SIGKDD Conference on Knowledge Discovery and Data Mining*.
- Zheng, J.; He, K.; and Zhou, J. 2023. Farsighted probabilistic sampling: A general strategy for boosting local search MaxSAT solvers. In *Proceedings of the AAAI Conference on Artificial Intelligence*, volume 37, 4132–4139.
- Zhou, Q.; Benlic, U.; and Wu, Q. 2020. An opposition-based memetic algorithm for the maximum quasi-clique problem. *European Journal of Operational Research*, 286(1): 63–83.